

Louisiana Wetland Water Level Monitoring Using Retracked TOPEX/POSEIDON Altimetry

HYONGKI LEE,¹ C. K. SHUM,¹ YUCHAN YI,¹
MOTOMU IBARAKI,¹ JIN-WOO KIM,¹ ALEXANDER
BRAUN,² CHUNG-YEN KUO,³ AND ZHONG LU⁴

¹School of Earth Sciences, The Ohio State University, Columbus, Ohio, USA

²Department of Geomatics Engineering, University of Calgary, Calgary, Canada

³Department of Geomatics, National Cheng Kung University, Tainan, Taiwan

⁴U.S. Geological Survey, Vancouver, Washington, USA

Previous studies using satellite radar altimetry to observe inland river and wetland water level changes usually spatially average high-rate (10-Hz for TOPEX, 18-Hz for Envisat) measurements. Here we develop a technique to apply retracking of TOPEX waveforms by optimizing the estimated retracked gate positions using the Offset Center of Gravity retracker. This study, for the first time, utilizes stacking of retracked TOPEX data over Louisiana wetland and concludes that the water level observed by each of 10-Hz data with along-track sampling of ~660 m exhibit variations, indicating detection of wetland dynamics. After further validations using nearby river gauges, we conclude that TOPEX is capable of measuring accurate water level changes beneath heavy-vegetation canopy region (swamp forest), and that it revealed wetland dynamic flow characteristics along track with spatial scale of 660 m or longer.

Keywords Satellite radar altimetry, Louisiana wetlands, water level change, waveform retracking, *stackfile*

1. Introduction

Coastal estuaries, which connect coastal ocean, wetlands, and land region, play an important role in ecology and environments in coastal regions. Wetlands typically occur in low-lying areas on the edges of lakes and rivers, or in coastal areas protected from waves. These wetlands are found in a variety of climates on every continent except Antarctica. Wetlands not only provide habitat for thousands of aquatic/terrestrial plant and animal species but also control floods by holding water like a sponge and reducing the velocity of storm water. Human activities have many negative impacts on wetlands and have become the main contributing factors to wetlands loss. Wetland loss is also caused by natural processes such as subsidence. Louisiana's wetlands, one of the largest expanses of coastal wetland in the United States, have lost about 100–150 km² of its area per year, and the loss rate

Received 29 December 2008; revised and accepted 4 June 2009.

Address correspondence to Hyongki Lee, Division of Geodetic Sciences, School of Earth Sciences, The Ohio State University, 275 Mendenhall Laboratory, 125 South Oval Mall, Columbus, Ohio 43210. E-mail: lee.2444@osu.edu

is increasing exponentially (Walker et al. 1987; Templet and Meyer-Arendt 1988). The vertical crustal motion, or subsidence in coastal Louisiana, is one of the primary reasons for wetland loss. The geological subsidence is due primarily to the loading inundation of ~130 m due to sea level rise at 21–5 kyr BP (thousands of years before present) and the Pleistocene sediment transport deposition to the Gulf of Mexico (Ivins et al. 2007). The equilibrium between the substrate surface and the relative sea level should be maintained to prevent land loss and marine transgression, which are anticipated where aggradation is less than the relative sea level rise (Hatton et al. 1983). Therefore, the rising sea level together with the subsidence accelerates the coastal erosion and wetland loss. Furthermore, it also aggravates the occurrence of flooding from the severe storm surge such as the devastating 2005 Hurricane Katrina.

The ability to quantitatively measure accurate wetland water level changes in Louisiana is critical for ecology and natural hazards mitigation, including improved storm surge modeling. Nevertheless, the water level gauging stations can be scarce or even absent in the floodplain/wetland due to the difficulty in physical access to the sites and logistics in data gathering. Hence, satellite all-weather remote sensing can provide useful measurements to monitor the water level variation over those regions. Interferometric Synthetic Aperture Radar (InSAR) has been useful in measuring cm-scale relative water level changes over the Amazon flood plain (Alsdorf et al. 2000, 2001) and the Everglades wetland (Wdowinski et al. 2004) using L-band SAR imagery. This is based on the fact that flooded forests permit double-bounce returns allowing InSAR coherence to be maintained. Furthermore, it has been demonstrated that the higher resolution ERS-1/2 C-band InSAR data have been used to accurately monitor water level changes over Louisiana wetlands (Lu et al. 2005; Lu and Kwoun 2008). In addition, satellite radar altimetry has been used to measure inland water level variation over large river basins (Birkett 1998; Alsdorf et al. 2001; Birkett et al. 2002; Maheu et al. 2003; Frappart et al. 2006).

In this study, decadal (1992–2002) TOPEX/POSEIDON data are used to measure water level changes over Louisiana vegetated wetlands. Unlike previous studies, which spatially averaged 10-Hz data (or 18-Hz for ERS-1/2 and ENVISAT altimetry) over a distance corresponding to the intersection between the satellite ground track and the water body, the “stacking” of 10-Hz data (Lee et al. 2008), or the so-called *stackfile* technique (Sandwell and Zhang 1989; Shum et al. 1990; Kruizinga 1997; Yi 2000), is used over Louisiana wetlands. Our technique allows us to measure water level changes over each 10-Hz *stackfile* bin, which has an along-track ground spacing of ~660 m (the nominal pulse-limited radar altimetry footprint is a few km), and leads us to obtain much finer along-track spatial sampling compared to the previous studies. The feasibility of applying optimal retracking correction is also demonstrated via validations with *in situ* river gauge data, whereas previous studies (Birkett 1998; Alsdorf et al. 2001; Birkett et al. 2002; Maheu et al. 2003) considered radar returns from nominal tracking mode contained in TOPEX Geophysical Data Records (GDRs) adequate.

2. Data

In this study, TOPEX GDRs and Sensor Data Records (SDRs) for (10 sidereal day repeat) cycle 9 through cycle 364 are used. The POSEIDON data are not used. The TOPEX GDRs and SDRs are available from the NASA/JPL Physical Oceanography Distributed Active Archive Center (PO.DAAC). We utilize the Ku-band 10-Hz range data contained in GDRs, and their respective 10-Hz geodetic coordinates per each cycle are computed using the

Precise Orbit Ephemeris (POE) data provided by NASA Goddard Space Flight Center (GSFC) (N. Zelensky, personal communication) using the 10-Hz time tags calculated from the 20-Hz range measurements contained in SDRs. Detailed description of the SDR data records can be found in Algiers et al. (1993). The SDRs also contain 10-Hz 64-sample waveform measurements, which are used for waveform retracking. The waveform anomalies such as zero-leakage and the offset leakage effects are mitigated by employing the sets of multiplicative and additive waveform factors (Hayne et al. 1994). The instrument corrections, media corrections (dry troposphere correction, wet troposphere correction calculated by the French Meteorological Office (FMO) from the European Centre for Medium-range Weather Forecasts (ECMWF) model, and the ionosphere correction based on onboard DORIS measurements), and geophysical corrections (solid Earth and pole tide) have been applied. The ionosphere corrections usually obtained by combining the dual-frequency altimeter measurements over ocean could not be used in this study because of land contaminations. Thus, the DORIS ionosphere corrections in the GDR are used in this study.

The river gauge data used in this study can be accessed from the United States Army Corps of Engineers. All available river gauge stations are illustrated as red triangles in Figure 3.

3. Methodology

3.1. 10-Hz Stackfile

The altimeter *stackfile* database structure was first developed by the Center for Space Research (CSR), University of Texas to efficiently access, store and process the spaceborne radar altimetry measurements over global ocean (Sandwell and Zhang 1989; Shum et al. 1990; Kruizinga 1997). The *stackfile* can be viewed as a three-dimensional array. The three dimensions denote (1) the distance from the equator along an orbit (row number), (2) orbit number of a repeat cycle (column number, or an equator-crossing longitude), and (3) the specific repeat cycle. Data are stored into bins, whose along-track dimension approximately corresponds to one second of time along the satellite ground tracks. A bin contains all the information from various repeat cycles measured over a particular area of the earth. The bins are addressed with row and column indices. Each column corresponds to a particular pass or orbit, and each row corresponds to particular latitude. More detailed information about the *stackfile* can be found in Kruizinga (1997). Although the established procedure in this study pertains to the processing of TOPEX/POSEIDON data, the procedure is applicable to efficient processing of any other satellite altimetry data.

In this study, a TOPEX 10-Hz regional *stackfile* over Louisiana wetlands is developed using an on-the-fly procedure instead of storing the data on each *stackfile* bin, as the conventional 1-Hz ocean *stackfile* does. First, a skeleton of 1-Hz regional *stackfile* over Louisiana is built based on the Ohio State University (OSU) *stackfile* software (Yi 2000). In other words, an empty three-dimensional array is constructed, and each bin in the array is assigned to a particular cycle, pass, and record of TOPEX GDRs (and SDRs) to perform the collinear analysis. For each GDR record from the given TOPEX cycle and pass, the corresponding row is predicted based on an equator crossing table, which is computed by interpolating the precision orbit ephemeris (POE) of TOPEX. The equator crossing tables are the basis of mapping transformation between time tags in GDR record and row-column addresses of 1-Hz *stackfile* bins. If the predicted 1-Hz *stackfile* row-column address is equivalent to the given bin address of the empty *stackfile* array, then for each

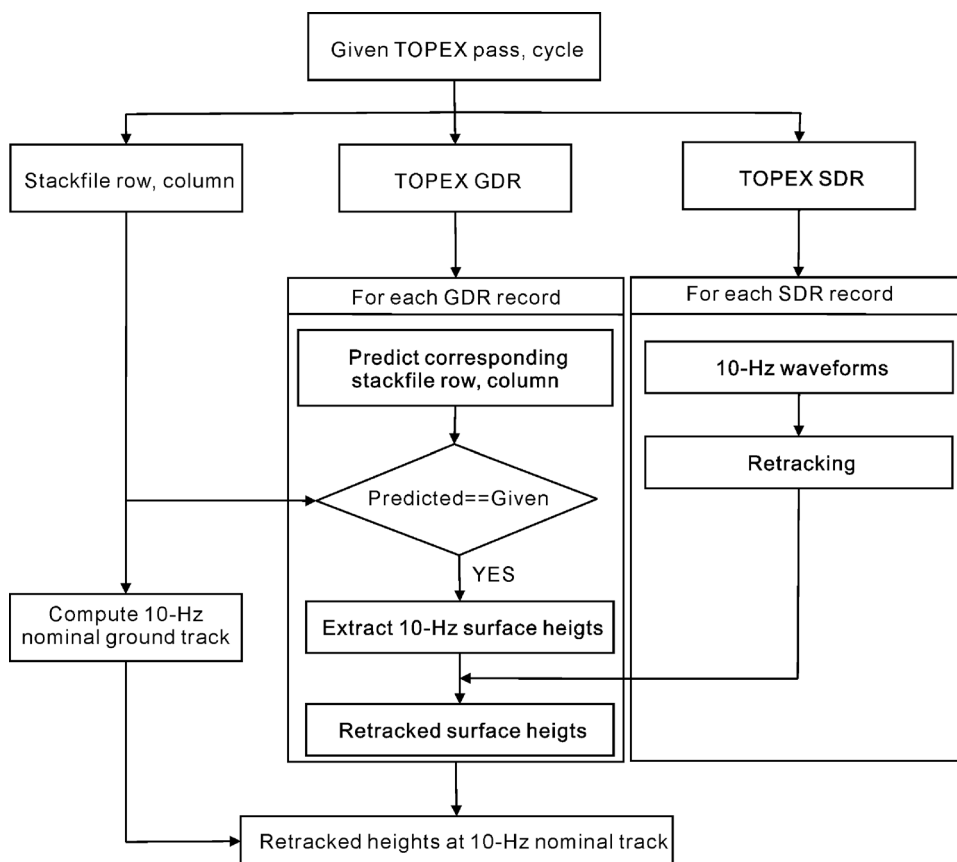


Figure 1. Diagram for the TOPEX 10-Hz *stackfile* procedure used in this study.

1-Hz *stackfile* bin, 10-Hz *stackfile* bins (or 10-Hz nominal ground tracks) are created by the procedures described in Lee et al. (2008). Next, each of 10-Hz range measurements contained in TOPEX GDRs can be assigned to each corresponding 10-Hz *stackfile* bin. The 10-Hz range measurements can be further corrected by applying retracking corrections using the waveform data contained in TOPEX SDRs (see Section 3.3). Finally, we construct a time series of water level changes over each 10-Hz *stackfile* bin or more than one 10-Hz *stackfile* bin by spatially averaging the data. Figure 1 shows a flowchart for the 10-Hz *stackfile* procedure developed and used in this study. In our procedure, not only 10-Hz range measurements but also any 10-Hz observations such as Automatic Gain Control (AGC) or pulse peakiness (see Section 3.2) can be simultaneously processed.

3.2. Target Selection

The study area includes the Teche/Vermillion Basin (Area1 and Area2), Barataria Basin (Area3), Lake Pontchartrain Basin (Area4), and Atchafalaya Basin (Area5) of coastal Louisiana wetland region (Figures 2 and 3). Geographic boundaries of the study areas are selected using the land classification map from Louisiana Gap Analysis Program (GAP) by including only marsh regions that are intersected by the satellite passes and excluding

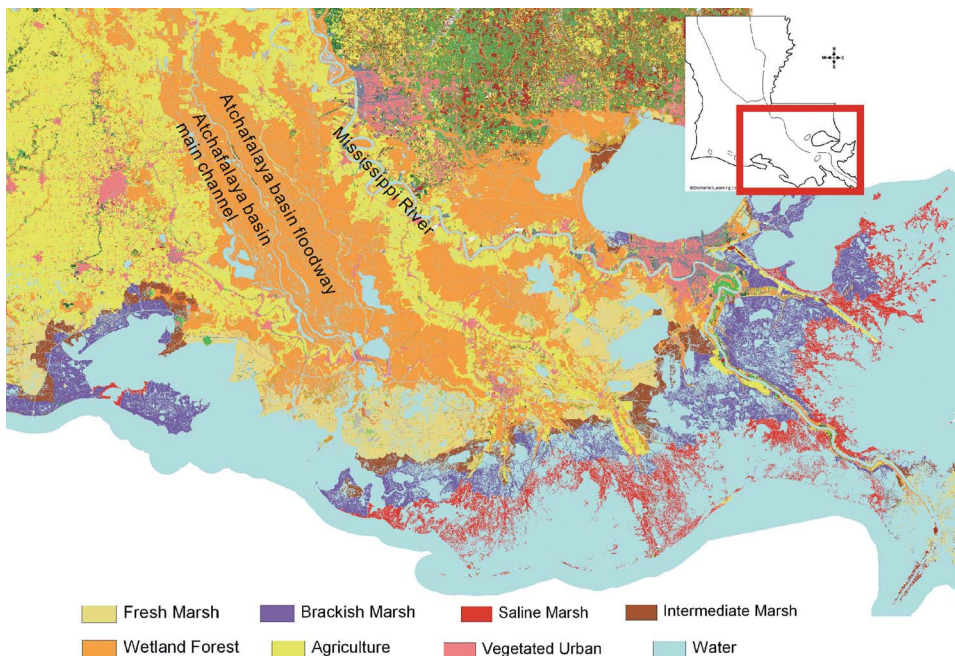


Figure 2. Classification map from GAP, showing major land cover classes of the study area.

agricultural cropland/grassland. The land cover classification map from GAP is shown in Figure 2. According to the land cover map from the Louisiana GAP project and other studies (Visser et al. 1998, 2000), the vegetation type of Area1 and Area2 is brackish marsh, of which the measured mean mudline elevation is approximately 28 cm (Gammill et al. 2002). Area3 and Area4 are covered by saline marshes, which are adjacent to the bays. Area5, upstream Atchafalaya Basin, is covered by swamp forest, which is composed of moderately dense trees ranging from 10–25 m in height (Lu et al. 2005; Lu and Kwoun 2008). Figure 3 illustrates the study areas with TOPEX tracks, and the detailed description is given in Table 1.

Table 1
Details of the study areas

	Geographic Range, deg (lat, lon) to (lat, lon)		Pass	Gauge		Distance to gauge (km)	Vegetation
				ID	Name		
Area1	(29.574, -92.202)	(29.702, -92.136)	117	76592	Fresh Water North	16	Brackish Marsh
Area2	(29.732, -92.120)	(29.860, -92.054)	117	76720	Leland Bowman East	11	Brackish Marsh
Area3	(29.325, -89.495)	(29.386, -89.463)	193	01480	Venice	15	Saline Marsh
Area4	(29.853, -89.355)	(29.919, -89.389)	204	85800	Shell Beach	30	Saline Marsh
Area5	(30.373, -91.759)	(30.572, -91.681)	117	49255	Bayou Fordoche	9	Swamp
				03075	Krotz Springs	7	Forest

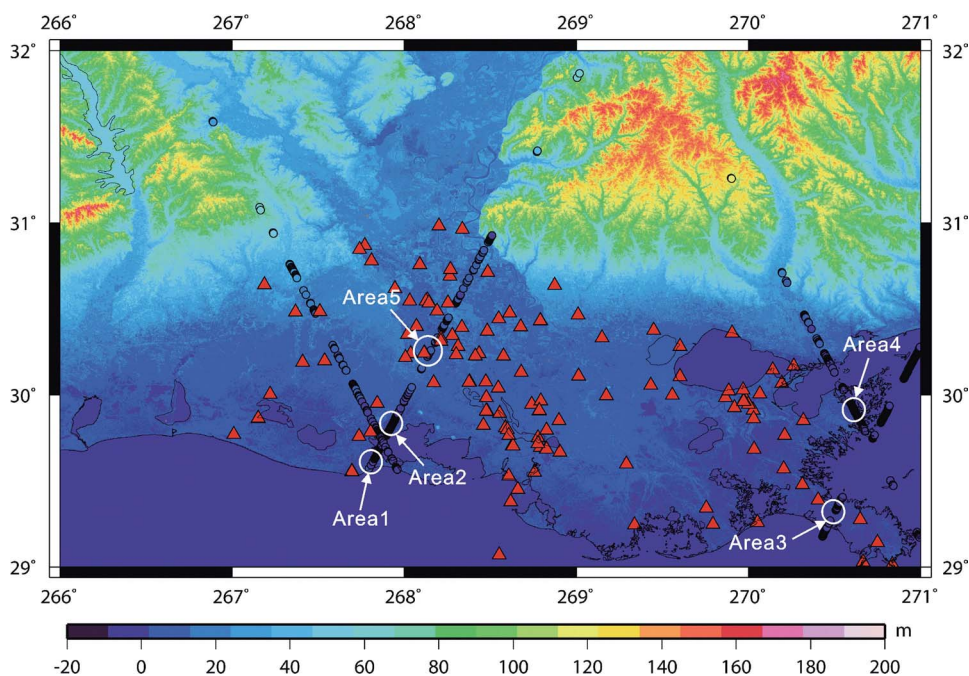


Figure 3. Map of Louisiana with TOPEX 10-Hz ground track of cycle 270. Background is SRTM C-band 90-meter resolution DEM, and red triangles represent river gauge stations, which can be accessed from the United States Army Corps of Engineers at <http://www.mvn.usace.army.mil/eng/edhd/Wcontrol/wcmain.htm>.

To identify “water-covered” surface, a test is performed based on pulse peakiness (PP) (Strawbridge and Laxon 1994) computed from 10-Hz waveform and 10-Hz Automatic Gain Control (AGC) parameter contained in TOPEX SDRs. This is the similar procedure described in Birkett (1998) except that we utilize the 10-Hz AGC value assigned to each corresponding 10-Hz *stackfile* bin instead of 1-Hz backscattering coefficient (σ_0) obtained from TOPEX GDRs because our goal is to distinguish or classify every 10-Hz range measurement of water surface from that of vegetation. As Area1, Area3, and Area4 are surrounded by the ocean, the PP and AGC values obtained over wetland are thus compared to the values over the ocean. On the other hand, Area2 and Area5 are located near agricultural cropland/grassland. Hence, the PP and AGC values are used to distinguish these features from water or ocean. Figure 4 illustrates the AGC versus PP values obtained from TOPEX cycle 9 to 83 to include one-year of measurements within each study area. Each panel, that is, different types of land cover, in Figure 4 clearly shows distinct divisions between wetland and coastal ocean, or wetland and dry land. Hence, we are able to characterize corresponding wetland waveforms according to the different PP and AGC thresholds (Table 2), which have been determined differently from area to area.

Figure 5 (i) and (ii) panels (a)–(e), respectively, show the mean of AGC and PP values, computed from cycle 9 to 364, over each 10-Hz *stackfile* bin, and Figure 5 (iii) and (iv) panels (a)–(e) illustrate their respective standard deviations. We can clearly observe the spatial variation of the AGC and PP along the satellite ground track, and these may represent the spatial variation of the surface characteristics, that is, the variation of wetland water level or the vegetation canopy. As illustrated in Figure 4, in general, the AGC and

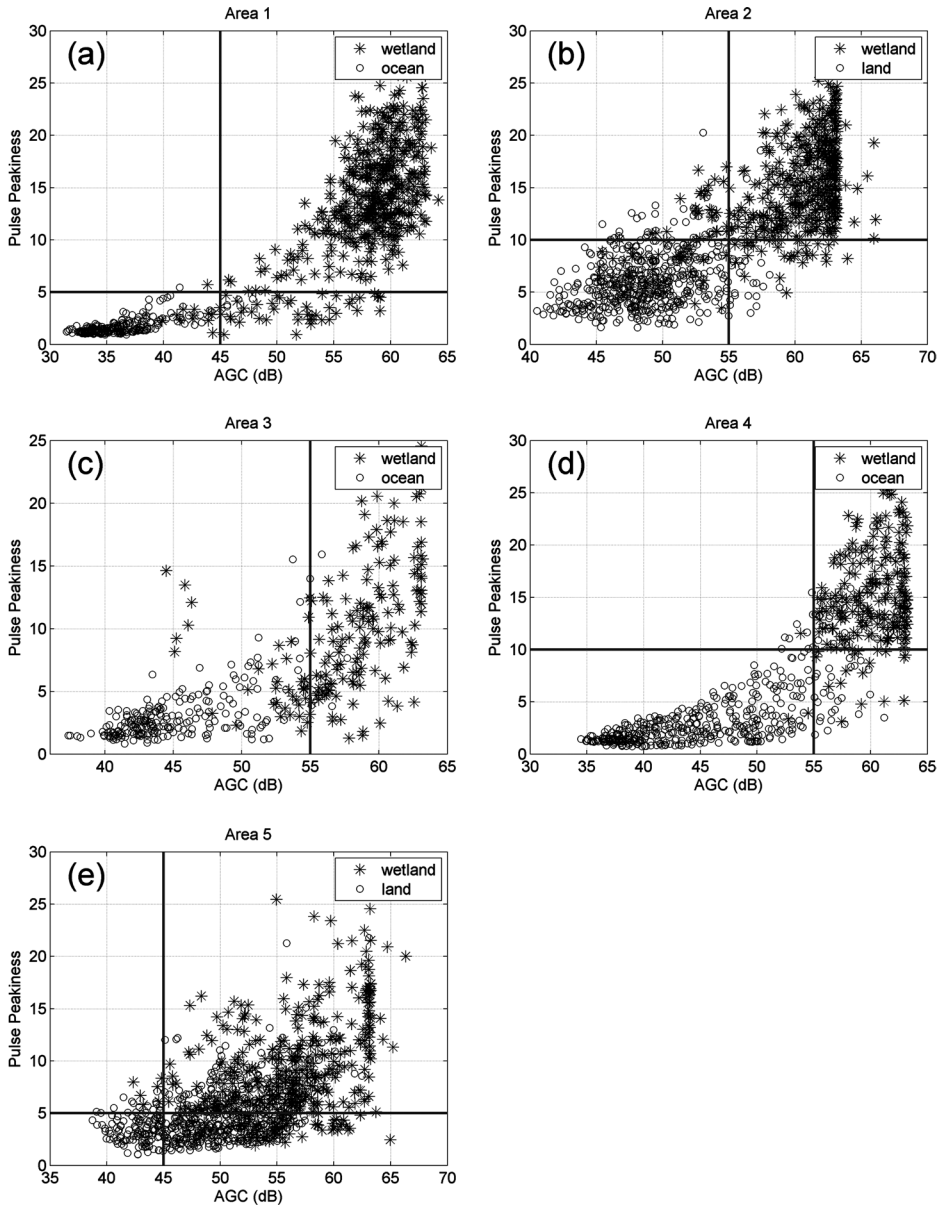


Figure 4. AGC versus PP plots over each study area. Thresholds of AGC and PP values to select possible water signals from the wetlands are indicated by straight lines. (a)~(e) correspond to Area1~Area5.

PP values show correlations between them. It can be seen from Figure 5 (i) and (iii) panels (a), (b), and (c) that the mean of AGC and PP values increase as the TOPEX ground track moves northward, which may indicate the presence of more water-covered wetland, and thus the radar return is dominated by surface water, not vegetation. It can also be seen from Figure 5 (ii) panels (a), (b), (c), and (d) that the standard deviation of AGC values decrease as the mean AGC values increase. Figure 5 (i) and (iii) for Area4 (d) show that low AGC

Table 2
Thresholds of AGC and PP values used to define
good wetland waveforms

	Area1	Area2	Area3	Area4	Area5
AGC	45	55	55	55	45
PP	5	10	—	10	5

and PP values at both ends whereas the middle of the study area shows higher AGC and PP values. This is because the radar waveform may contain signal from the coastal ocean. Over Area5 (Figure 5 (e)), the classified vegetation type is swamp forest, and it shows smaller variations in AGC and PP values compared to other study areas.

3.3. Waveform Retracking

Over nonocean surfaces, the altimeter range measurements could have errors due to the complex nature of the signal reflected from the surface. To minimize errors, various waveform retracking techniques have been developed to correct the deviation of the waveform leading edge from the nominal predetermined tracking gate. The water surfaceTable 2 in wetlands could result in specular radar returns; if the water surface is seasonally vegetated, irregular shape of radar waveforms will be obtained. These waveforms do not conform to the Brown (1977) model “standard” waveforms; hence, the retracking has been studied. Previous studies (Birkett 1998; Birkett et al. 2002; Maheu et al. 2003) used 10-Hz range measurements available in the GDRs without retracking. Birkett (1998) concluded that retracking may cause unacceptable additional noise for constructing water level time series. This can be explained from the fact that the average positions of the waveform peak were close to the nominal tracking gate (for TOPEX, it is 24.5), which means the satellite is tracking the true water surface and retracking is not needed. However, this could be true only over large water bodies such as the Great Lakes (Morris and Gill 1994) or large river basins such as the Amazon (Birkett et al. 2002). In this study, the leading edge positions of each 10-Hz waveform, using SDRs from cycle 9 to 364, along each 10-Hz *stackfile* bin using Offset Center of Gravity (OCOG) retracker (Bamber 1994) are estimated, and their variations are examined. Figure 6 shows an example of waveform shape variation along TOPEX ground tracks from cycle 49. Most of the waveforms over wetland are specular (or narrow-peaked) except for the waveforms around the boundary between the ocean and wetland, which are relatively more noisy (Figure 6 (a)).

Although narrow-peaked waveforms may provide stable water height at times of level maxima (Birkett 1998), the waveform shape over a 10-Hz *stackfile* bin may vary from cycle to cycle at times of level minima. This justifies the need for retracking. The variation of the retracked gate positions are shown in the box-plot of Figure 7 using the waveforms, which satisfies the editing criteria using AGC and PP values. Area1_1 means the southernmost 10-Hz *stackfile* bin of Area1, Area1_2 means the next 10-Hz *stackfile* bin of Area1, and so on. Study sites of Area1_14, Area1_15, Area1_16, Area2_10, Area2_11, Area2_15, and Area4_11 are arbitrarily chosen among the study sites which show smaller variation in the position of retracked gate, and thus retracking may not be applied. Area3_6, Area3_9, Area5_15, Area5_17, Area5_18, Area5_19, and Area5_22, which are marked with ellipses

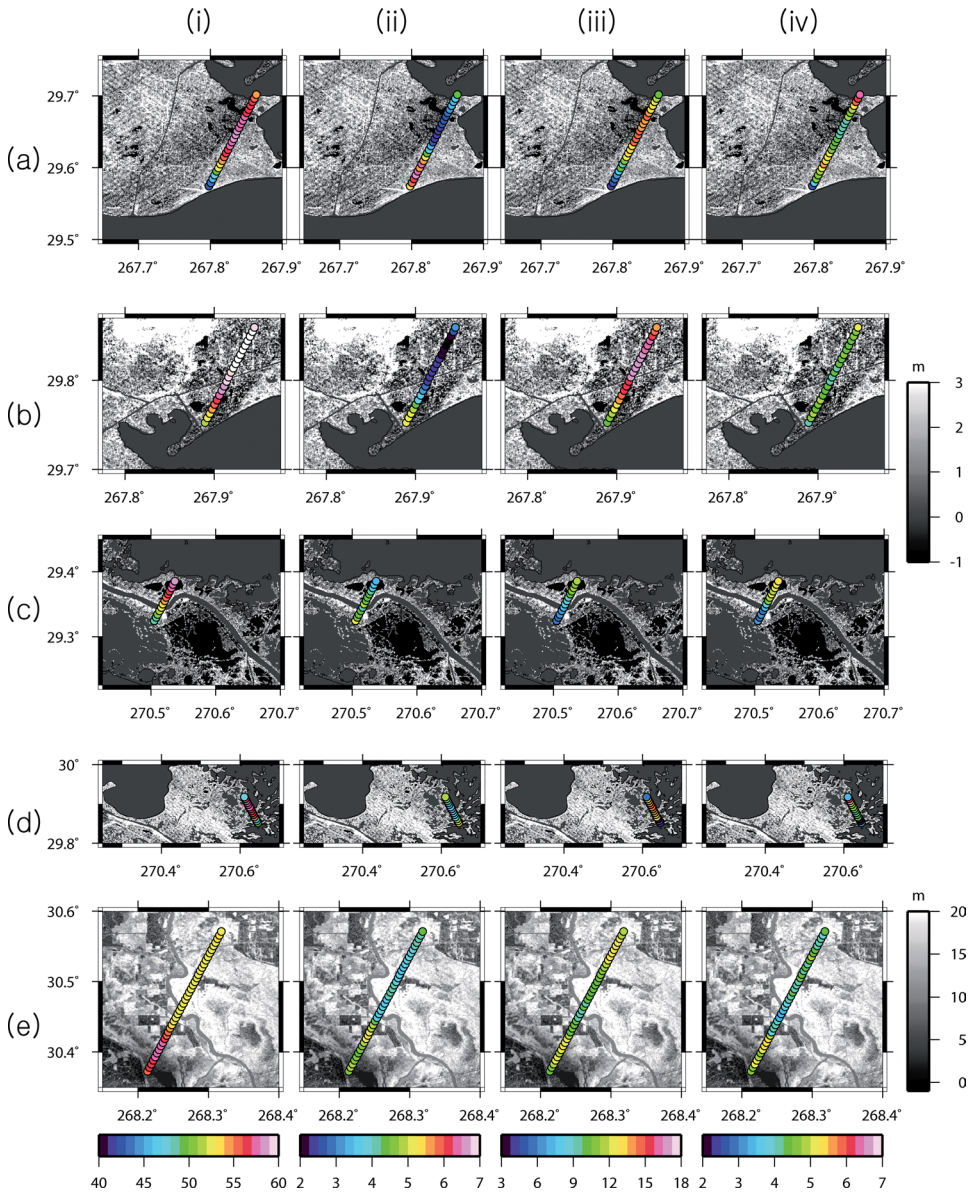
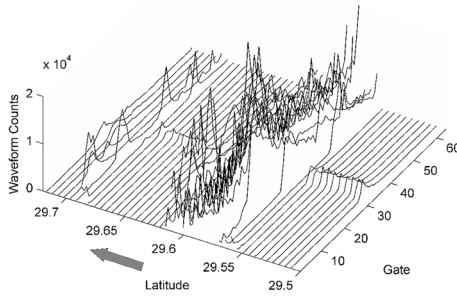


Figure 5. (i) Averages of AGC (dB), (ii) standard deviations of AGC (dB), (iii) averages of PP, (iv) standard deviations of PP over each 10-Hz *stackfile* bin of Area1 to Area5 ((a)~(e)). The background is SRTM DEM elevation (m) with its color-bar on the right side. A common color-bar is used for Area1 to Area4. The Mississippi River and Atchafalaya River can be seen in Area3 and Area5, respectively.

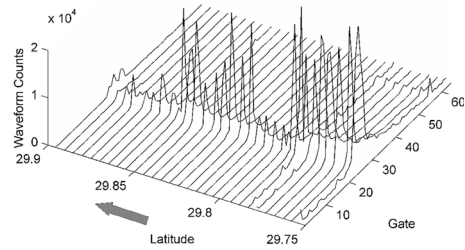
in the figure, represent the study sites whose variations of the retracked gates are large. This indicates the need for retracking.

To further justify the need for retracking, the correlation coefficient (CC) and root-mean-square (RMS) difference between the water level time series from TOPEX and the

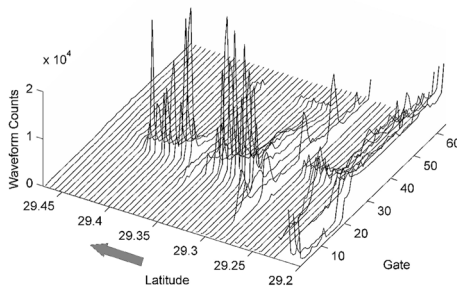
(a) Area1, Pass117



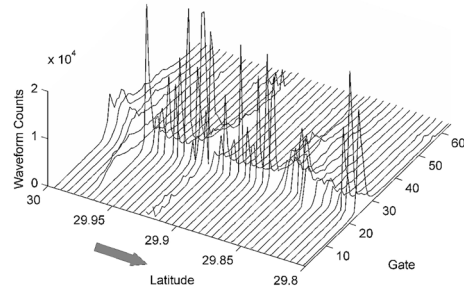
(b) Area2, Pass117



(c) Area3, Pass193



(d) Area4, Pass204



(e) Area5, Pass117

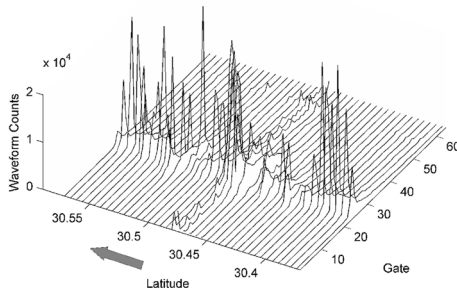


Figure 6. Variations of waveform shapes along satellite ground track from cycle 49. The high-peaked specular responses may indicate the presence of calm water in vegetated wetland. The arrow beside the axis of latitude indicates the direction of the satellite flight along the ground track.

nearby river gauge are examined. Original river gauge data are daily measurements whereas the TOPEX data sampling interval is 10 days. Therefore, each river gauge measurement closest in time to the TOPEX 10-day repeat measurement is selected to compute CC and RMS differences. It should be noted that the water level anomalies from TOPEX and river gauges are compared as they have different datum. Figure 8 shows the comparison between the water level time series constructed from TOPEX and river gauge measurements over study sites Area3.6, Area3.9, Area5.15, Area5.17, Area5.18, Area5.19, and Area5.22 before and after retracking. As expected, while the study sites with smaller variation in the position of the retracked gate show no significant improvement after retracking,

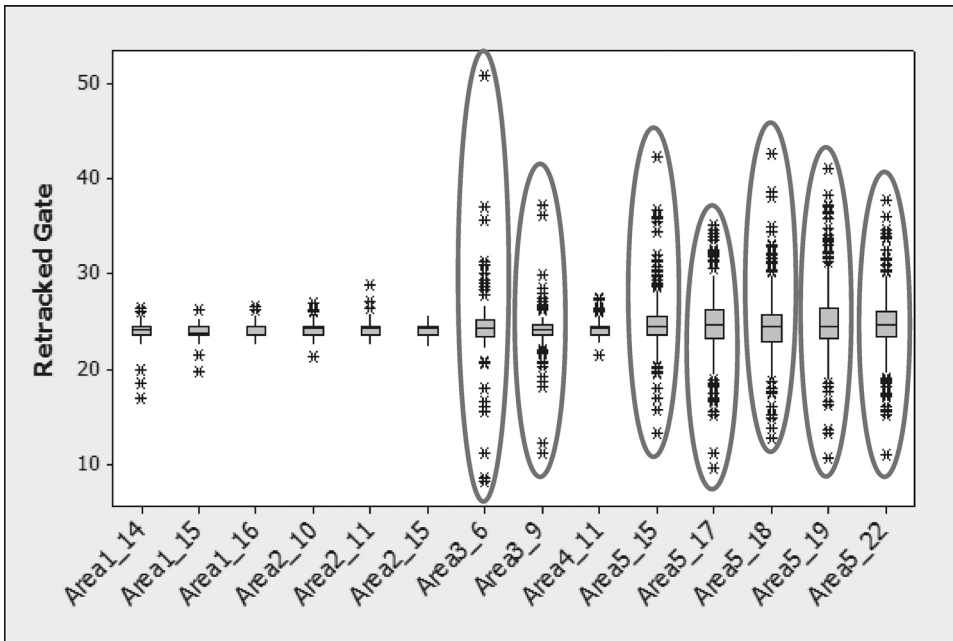


Figure 7. Box-plot of retracked gates obtained from OCOG retracker. Area1_1 means the southernmost 10-Hz *stackfile* bin of Area1, Area1_2 means the next 10-Hz *stackfile* bin of Area1, and so on. Area3_6, Area3_9, Area5_15, Area5_17, Area5_18, Area5_19, and Area5_22 (marked with ellipses) show larger variation of retracked gates than other study sites. The study sites with larger variations of retracked gates showed higher correlation coefficient and smaller RMS differences between TOPEX and river gauge water level change time series after applying retracking (see Figure 8).

the study sites with larger variation in the waveform leading edge position show higher correlation coefficients and smaller RMS differences after retracking. Hence, we conclude that the possible need for retracking should be checked for inland hydrologic application of satellite radar altimetry, in particular, over vegetated wetlands. Figure 9 (i) panels (a)–(e) show the spatial variation of CC, and it can be seen from the figure that CCs of the 10-Hz *stackfile* bins, which are geographically close to the river gauges, are not necessarily high. This phenomena may indicate the complex nature of the wetland water flow dynamics, as can be seen from Figure 9 (a)(i) and (b)(i). In Area3 (Figure 9 (c)(i)), the 10-Hz *stackfile* bin, which is closest to the Mississippi River, shows the highest CC after retracking. It is also interesting to note that Area5 (Figure 9 (e)(i)), whose vegetation type is swamp forest, shows generally high correlation coefficients. This shows the capability of Ku-band radar altimeter to measure changes in water level beneath the tree/vegetation cover, indicating that the altimetry water level height measurements are indeed novel. According to Lu et al. (2005), whose study area is located in downstream of the Atchafalaya River, the swamp forests are composed of moderately dense trees ranging from 10–25 m in height with a medium-low canopy closure. Because the vegetation type of Area5 and the study area of Lu et al. (2005) are classified to be the same as “Wetland Forest Deciduous,” we conclude that Ku-band altimetry can penetrate through 20–50% tree cover (see figure 1 (c) of Lu et al. (2005)).

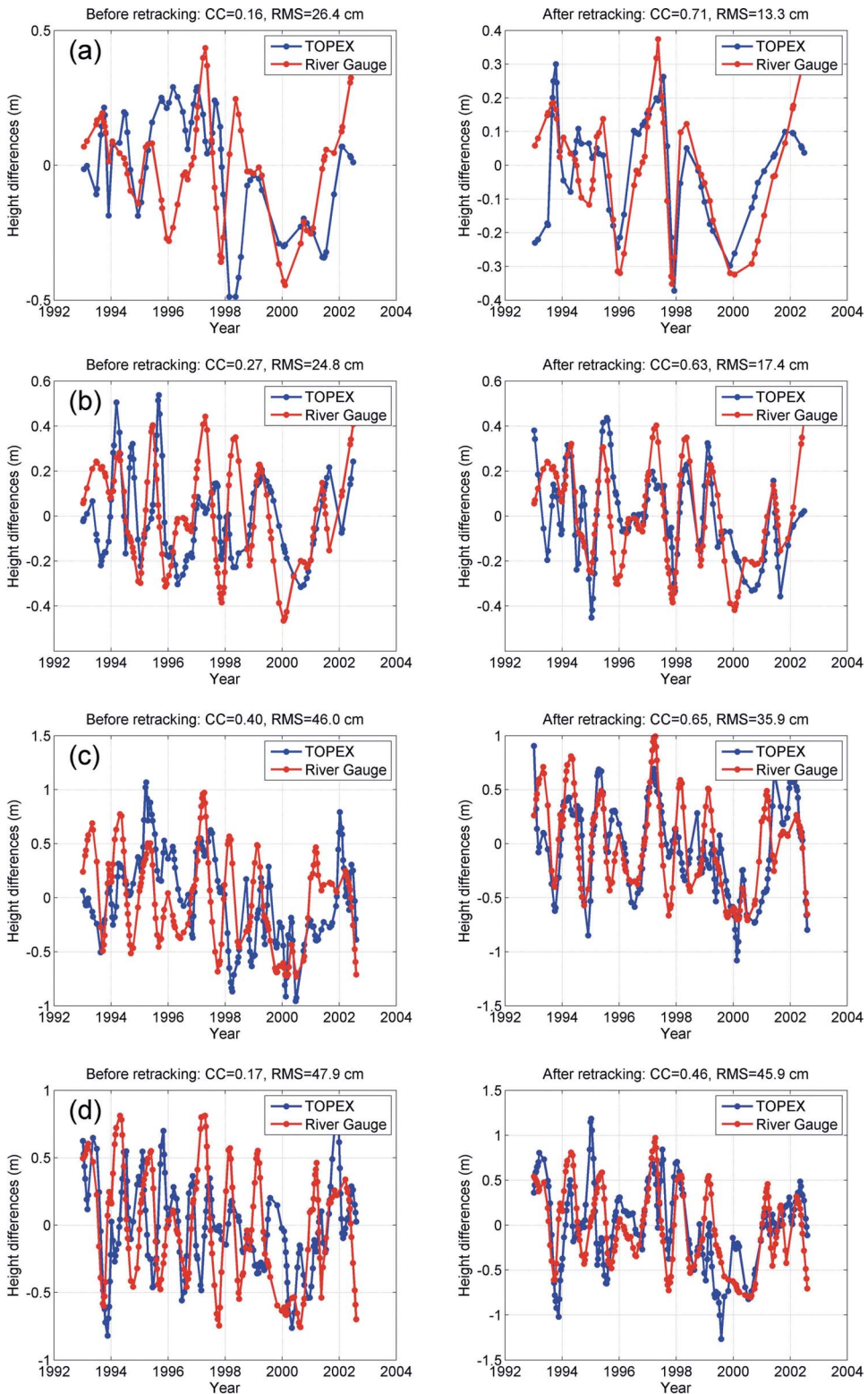


Figure 8. Comparison of TOPEX and nearby river gauge water level change time series before and after retracking over (a) Area3.6, (b) Area3.9, (c) Area5.15, (d) Area5.17, (e) Area5.18, (f) Area5.19, and (g) Area5.22, respectively. Note that higher correlation coefficient and smaller RMS differences are obtained after retracking. (*Continued*)

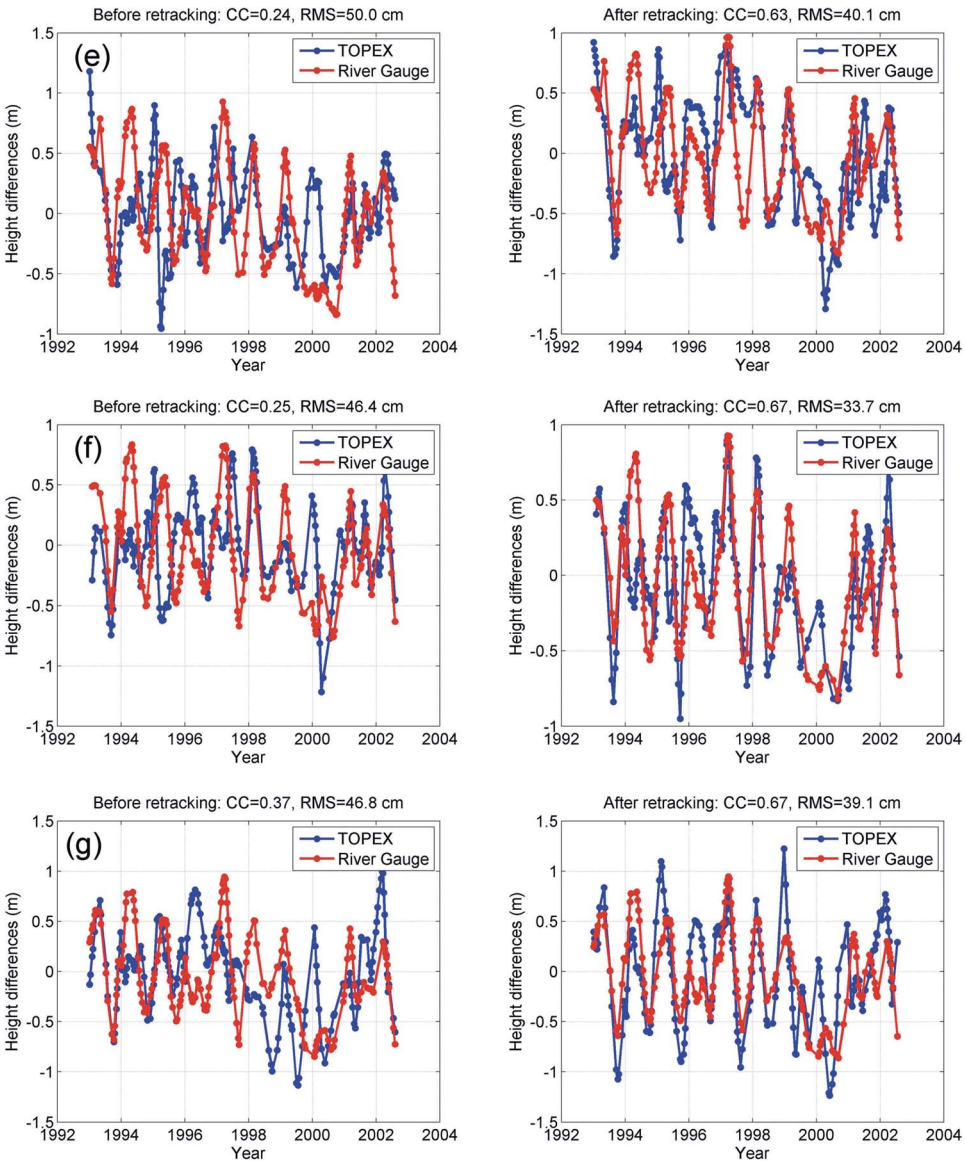


Figure 8. (Continued)

4. Results

As illustrated in Figure 3, a TOPEX track covers Area1, Area2 (brackish marsh), and Area5 (swamp forest), and the water level of Area5 shows much greater fluctuation than those of Area1 and Area2 (Figure 9). This is because these two areas are located in different hydrologic system. The brackish marsh regions (Area1 and Area2) are located next to the Vermillion bay and there is no big river in the area. The water level change, hence, is mainly affected by groundwater which interacts with surface water that is measured by TOPEX. Groundwater flow in the marsh area is influenced by regional groundwater flow system

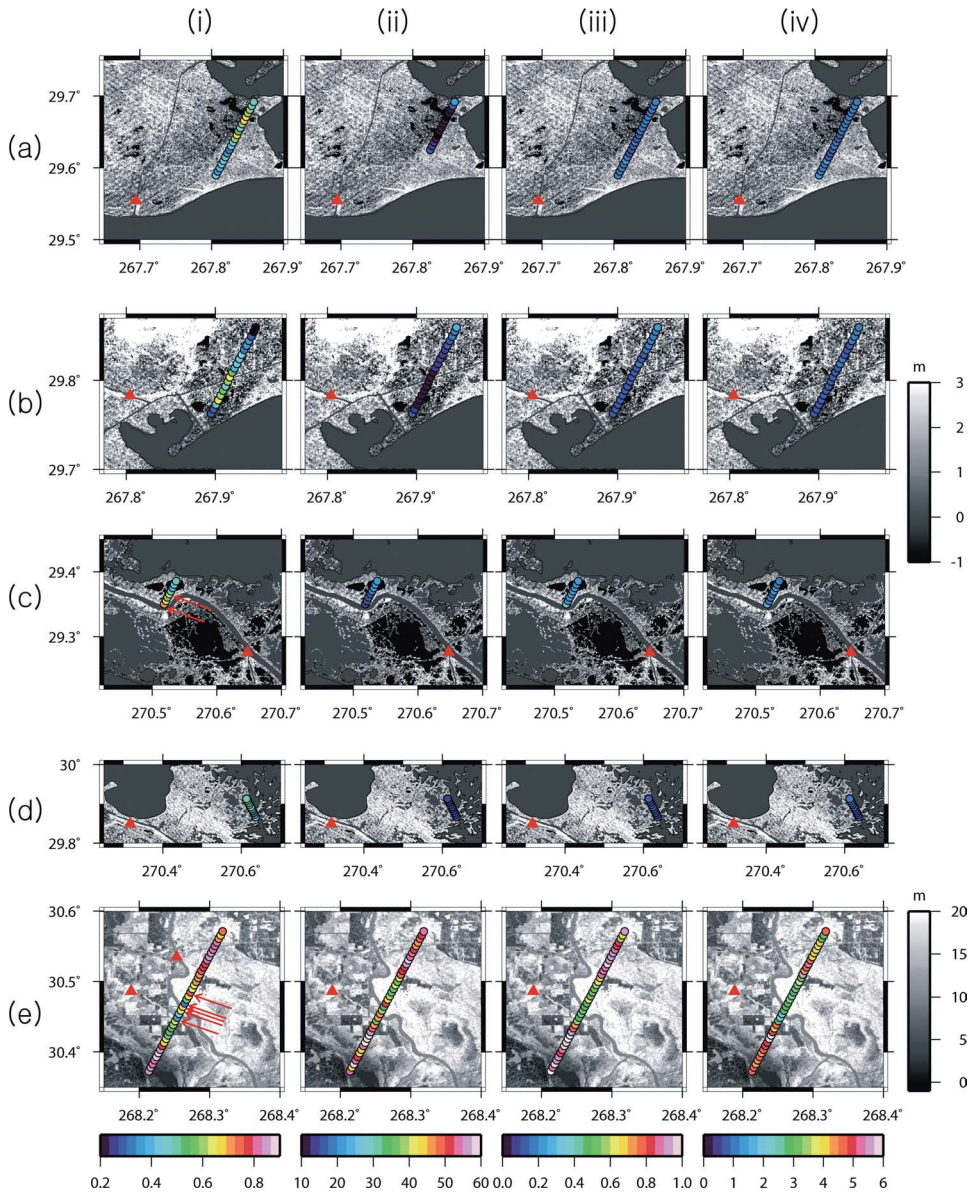


Figure 9. (i) Correlation coefficients and (ii) RMS differences (cm) between TOPEX and nearby river gauge (red triangle) water level change time series, (iii) stand deviations (m) and (iv) peak-to-peak amplitudes (m) of the TOPEX water level change time series over each 10-Hz *stackfile* bin. The *stackfile* bins, which showed improvement after retracking are indicated by red arrows. Background is the SRTM C-band DEM.

which can show seasonal changes. In contrast, the swamp forest area (Area5) is located next to the Atchafalaya River. The Atchafalaya River is a distributary of the Mississippi and Red rivers and provides a significant industrial shipping channel for the state of Louisiana. The U.S. Army Corps of Engineers maintains the river as a navigable channel of the Mississippi

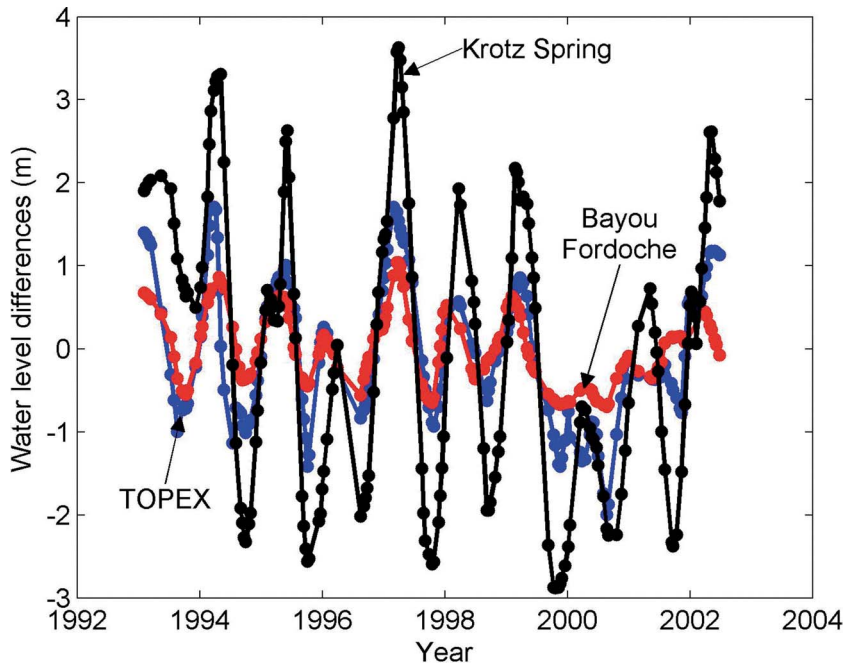


Figure 10. Water level change time series obtained over the study site Area5.1 from Krotz Spring stage (black), Bayou Fordoche stage (red), and TOPEX (blue), respectively.

and has constructed a series of water control structures. The combination of human-control and natural variations leads to more water level fluctuations compared to those caused by the groundwater flow system, which mainly controls the water level in the brackish marsh area.

In Area5, there are two river gauge stations (Krotz Spring and Bayou Fordoche), which have records contemporary to TOPEX. The Krotz Spring is located directly at the Atchafalaya River channel, and the Bayou Fordoche is located southwest of the Krotz Spring (Figure 9 (e)(i)). Figure 10 illustrates a comparison between water level time series obtained over the study site Area5.1 from Krotz Spring stage, Bayou Fordoche stage, and TOPEX. As can be seen, the amplitudes of the seasonal variation between the time series from Krotz Spring and Bayou Fordoche differ significantly, and the amplitude of TOPEX time series is closer to but a little larger than that of Bayou Fordoche. The RMS differences between the time series from Krotz Spring and TOPEX, and Bayou Fordoche and TOPEX, are 117.7 cm and 52.9 cm, respectively. On the other hand, it is also observed that the phases of the seasonal water level variations from Krotz Spring, Bayou Fordoche, and TOPEX agree very well. Correlation coefficients between Krotz Spring and TOPEX, and Bayou Fordoche and TOPEX, are 0.83 and 0.85, respectively. Hence, the TOPEX time series obtained from each 10-Hz *stackfile* bin follows the seasonal variation of the water level changes, and the amplitude also agrees well with the Bayou Fordoche, not Krotz Spring, which is located at the main stream of the Atchafalaya River.

The spatial variations of AGC and PP values over Area5 have been shown in Figure 5 (e)(i) and (e)(ii), respectively. It can be seen from the figure that the AGC values are higher

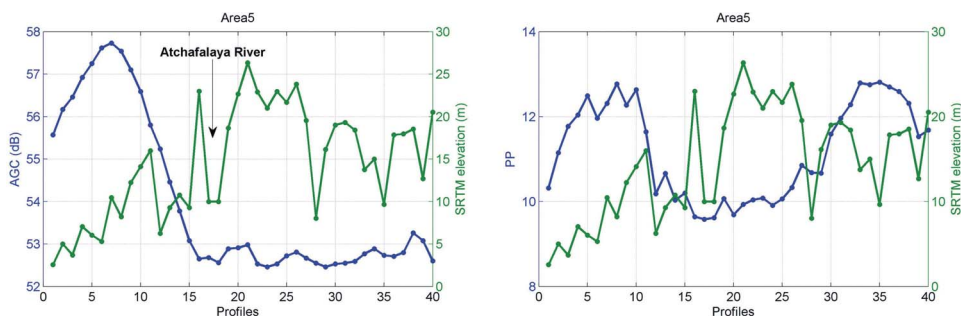


Figure 11. (a) AGC (dB), and (b) PP values and SRTM elevation along each 10-Hz *stackfile* bin over Area5, respectively.

over the southern part of Area5, and then start to decrease near the river channel and remain almost constant. On the other hand, the PP values are also higher over the southern part of Area5 and then decrease around the river channel. Unlike the AGC values, the PP values increase again around the northern part of Area5. As discussed in Section 3.2, both the AGC and PP values can be used to detect “water-covered” surfaces, and thus higher AGC and/or PP values may represent more flooded surface condition. In other words, the water level fluctuation over the southern part of Area5 can be larger than that over the northern part. To further validate the speculation, the Shuttle Radar Topography Mission (SRTM) C-band Digital Elevation Model (DEM) elevation is plotted in Figure 11 along with the AGC and PP values over each 10-Hz *stackfile* bin from south to north. From the SRTM elevation, it is clear that the higher river banks on both sides of the Atchafalaya River and the southern part has lower elevation than the northern part. Therefore, more flooded water will be found in southern part than the northern part, which resulted in higher AGC and PP values. In the next step, we examined the standard deviations and the peak-to-peak amplitudes of decadal TOPEX water level time series, which indicate water level fluctuation, over each 10-Hz *stackfile* bin. It can be seen from Figure 12 that both the standard deviations and the amplitudes of the 10-Hz TOPEX water level time series over the southern part are higher than those over the northern part. This observation demonstrates that the southern portion of Area5, which is located at the northern part of the swamp forest along the Atchafalaya River basin, is more flooded than the northern portion. However, it should be noted that

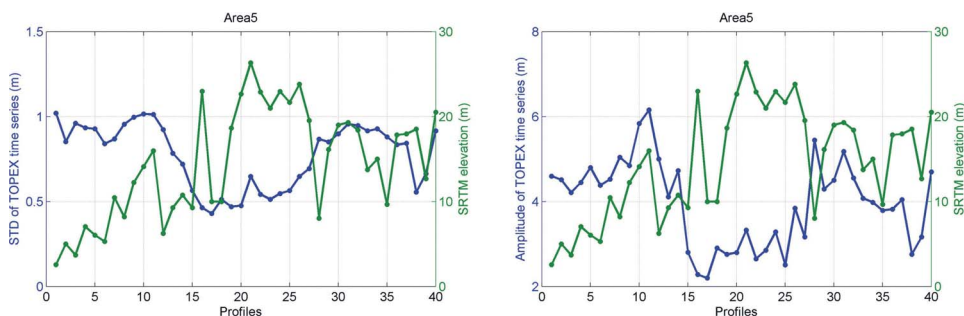


Figure 12. (a) Standard deviation (m), and (b) peak-to-peak amplitude (m) of TOPEX time series and SRTM elevation along each 10-Hz *stackfile* bin over Area5, respectively.

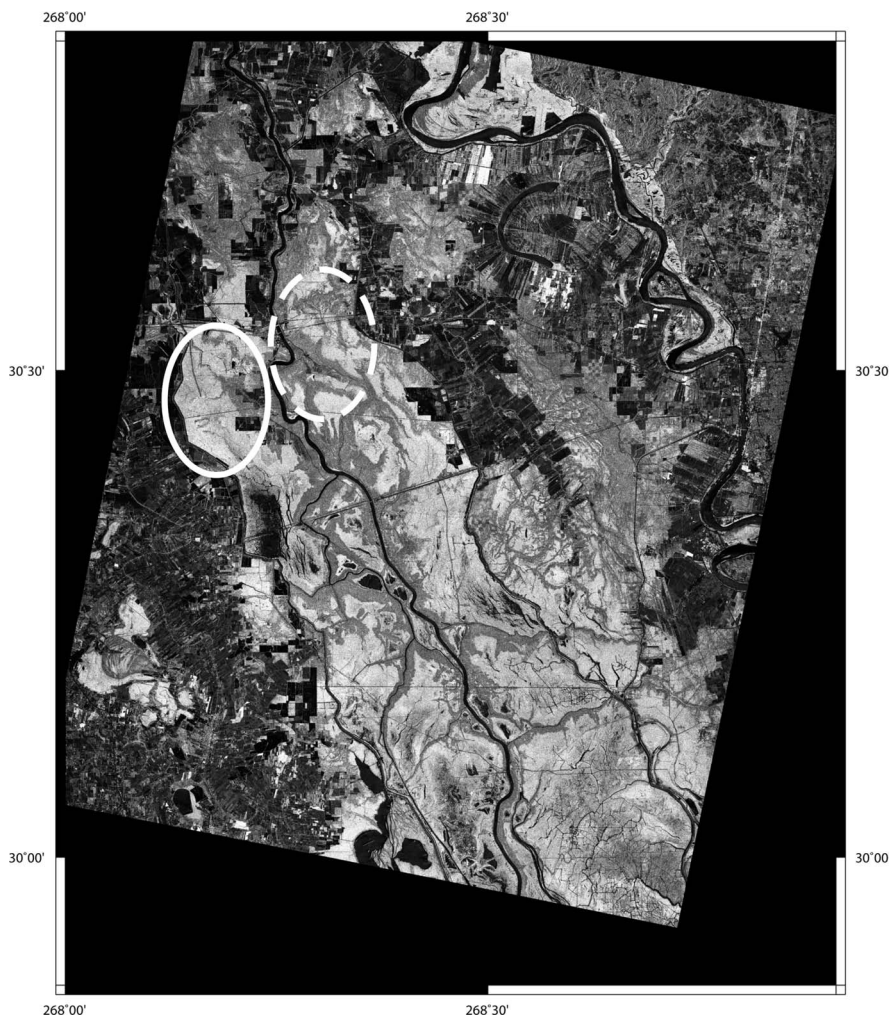


Figure 13. L-band ALOS SAR geocoded intensity image taken on Jan 29, 2007. The more flooded part in Area5 is marked with a solid circle, and the partially flooded part is marked with a dashed circle.

this can be local phenomenon only around Area5. This local phenomenon can be seen from the L-band Advanced Land Observing Satellite (ALOS) SAR geocoded intensity image, which was taken on January 29, 2007 and shown in Figure 13. According to Hess et al. (2003), the higher values in the L-band SAR intensity image may represent more flooded surface characteristics due to the so-called “double-bounce” scattering from the surface water and vegetation. It can be seen that the region shown with a solid circle shows higher intensity value than the region with a dashed circle. This agrees with our observation above.

It has been shown that TOPEX 10-Hz *stackfile* allows us to investigate wetland hydrology in higher spatial resolution with retracked altimeter measurements. The backscattered power, waveform shape, and water level change time series along each 10-Hz *stackfile* bin are used to characterize the local hydrologic conditions.

5. Conclusions

An innovative technique to estimate the water level variation using TOPEX radar altimetry in Louisiana wetlands was developed and demonstrated. The 10-Hz *stackfile* procedure was used to map the water level change over each of the 10-Hz *stackfile* bin with the highest along track spatial sampling (~660 m) achievable from TOPEX. This technique is different from the previous studies (Birkett 1998; Birkett et al. 2002; Maheu et al. 2003), which spatially averaged the 10-Hz measurements along the satellite track and river/wetland intersections, allowing only one time series per intersection. Furthermore, the need for retracking over vegetated wetlands was examined by computing the retracked gates and comparing the water level time series from TOPEX and river gauge before and after retracking. Study sites, which showed better agreement with the nearby river gauges, are located near the Mississippi River delta (Area3_6 and Area3_9) and around the swamp forest (Area5_15, Area5_17, Area5_18, Area5_19, and Area5_22). Most of the study sites, which did not show improvement after retracking, are distributed around the brackish marsh which has relatively low canopy.

None of the study areas showed higher correlation between the time series from TOPEX and river gauge, as the 10-Hz *stackfile* bins become closer to the river gauge station, which may indicate the complex nature of the wetlands flow dynamics due to the levees, dredging, and impoundment. Furthermore, it has been shown that the flooding characteristics over the both sides of the Atchafalaya River in Area5 are different, and the observation was explained using the SRTM DEM elevation.

These observations could help to quantify the depletion or rise of water level in wetlands and to provide precise estimates of water storage over wetlands. These observations also can be used to improve the hydrologic modeling by providing large-scale calibration datasets to precisely estimate hydrological parameters for numerical modeling. Improving hydrological modeling is a critical step to enhance prediction and assessment capabilities for future flood events over wetlands.

Acknowledgments

This research is partially supported by grants from the National Geospatial-Intelligence Agency's University Research Initiatives Program: HM1582-07-1-2024, National Science Foundation Hydrology program: EAR-0440007, and the Climate, Water, and Carbon Program at the Ohio State University. The TOPEX/POSEIDON data products used in this study are from NASA/JPL PO-DAAC and CNES AVISO. We also thank two anonymous reviewers for their constructive comments which have improved the manuscript.

References

- Algiers, J. et al. 1993. TOPEX ground system software interface specification, vol. 2: Design (SIS-2), altimeter sensor data record (SDR)—alt SDR data. March, JPL D-8591, Rev. C.
- Alsdorf, D. E., J.M. Melack, T. Dunne, L. Mertes, L.L. Hess, and L.C. Smith. 2000. Interferometric radar measurements of water level changes on the Amazon floodplain. *Nature* 404:174–177.
- Alsdorf, D., C. Birkett, T. Dunne, J. Melack, and L. Hess. 2001. Water level changes in a large Amazon lake measured with spaceborne radar interferometry and altimetry. *Geophy. Res. Lett.* 28:2671–2674.
- Bamber, J.L. 1994. Ice sheet altimeter processing scheme. *Int. J. Remote Sens.* 15:925–938.
- Birkett, C. M. 1998. Contribution of the TOPEX NASA radar altimeter to the global monitoring of large rivers and wetlands. *Water Resour. Res.* 34:1223–1239.

- Birkett, C. M., L. A.K. Mertes, T. Dunne, M. H. Costa, and M. J. Jasinski. 2002. Surface water dynamics in the Amazon Basin: Application of satellite radar altimetry. *J. Geophys. Res.* 107, doi:10.1029/2001JD000609.
- Brown, G. S. 1977. The average impulse response of a rough surface and its applications. *IEEE Trans. Antennas Propag.* 25:67–74.
- Frappart, F., S. Calmant, M. Cauhopé, F. Seyler, and A. Cazenave. 2006. Preliminary results of ENVISAT RA-2-derived water levels validation over the Amazon basin. *Remote Sens. Environ.* 100:252–264.
- Gammill, S. et al. 2002. *Hydrologic investigation of the Louisiana Chenier Plain*. Baton Rouge, LA: Louisiana Department of Natural Resources.
- Hatton, R., R. DeLaune, and W. Patrick, Jr. 1983. Sedimentation, accretion, and subsidence in marshes of Barataria Basin, Louisiana. *Limnol. Oceanogr.* 28:494–502.
- Hayne, G. S., D. W. Hancock III, and C. L. Purdy. 1994. The corrections for significant wave height and attitude effects in the TOPEX radar altimeter. *J. Geophys. Res.* 99:24941–24955.
- Hess, L. L., J. M. Melack, E. M.L.M Novo, C. C.F. Barbosa, and M. Gastil. 2003. Dual-season mapping of wetland inundation and vegetation for the central Amazon basin. *Remote Sens. Environ.* 87:404–428.
- Ivins, E., R. Dokka, and R. Blom. 2007. Post-glacial sediment load and subsidence in coastal Louisiana. *Geophys. Res. Lett.* 34, doi:10.1029/2007GL030003.
- Kruizinga, G. J. 1997. Dual-satellite altimeter crossover measurements for precise orbit determination. PhD diss., University of Texas, Austin.
- Lee, H., C. K. Shum, Y. Yi, A. Braun, and C. Y. Kuo. 2008. Laurentia crustal motion observed using TOPEX/POSEIDON radar altimetry. *J. Geodyn.* 46:182–193.
- Lu, Z., M. Crane, O. Kwoun, C. Wells, C. Swarzenski, and R. Rykhus. 2005. C-band radar observed water level change in swamp forest. *Eos.* 86:141–144.
- Lu, Z., and O. Kwoun. 2008. Radarsat-1 and ERS interferometric analysis over southeastern coastal Louisiana: Implication for mapping water-level changes beneath swamp forests. *IEEE Trans. Geosci. Remote Sens.* 46:2167–2184.
- Maheu, C., A. Cazenave, and C. R. Mechoso. 2003. Water level fluctuations in the Plata Basin (South America) from TOPEX/POSEIDON satellite altimetry. *Geophys. Res. Lett.* 30, doi:10.1029/2002GL016033.
- Morris, C. S., and S. K. Gill. 1994. Evaluation of the TOPEX/POSEIDON altimeter system over the Great Lakes. *J. Geophys. Res.* 99:24527–24539.
- Sandwell, D. T., and B. Zhang. 1989. Global mesoscale variability from the Geosat Exact Repeat Mission: Correlation with ocean depth. *J. Geophys. Res.* 94:17971–17984.
- Strawbridge, F., and S. Laxon. 1994. ERS-1 altimeter fast delivery data quality flagging over land surfaces. *Geophys. Res. Lett.* 21:1995–1998.
- Shum, C. K., R. A. Werner, D. T. Sandwell, B. H. Zhang, R. S. Nerem, and B. D. Tapley. 1990. Variations of global mesoscale eddy energy observed from Geosat. *J. Geophys. Res.* 95:17865–17876.
- Templet, P., and K. Meyer-Arendt. 1988. Louisiana wetland loss: a regional water management approach to the problem. *Environ. Manage.* 12:181–192.
- Visser, J., C. Sasser, R. Chabreck, and R. Linscombe. 1998. Marsh vegetation types of the Mississippi river deltaic plain. *Estuaries.* 21:818–828.
- Visser, J., C. Sasser, R. Linscombe, and R. Chabreck. 2000. Marsh vegetation types of the Chenier Plain, Louisiana, USA. *Estuaries* 23:318–327.
- Walker, J., J. Coleman, H. Roberts, and R. Tye. 1987. Wetland loss in Louisiana. *Geogr. Ann.* 69:189–200.
- Wdowinski, S., F. Amelung, F. Miralles-Wilhelm, T. H. Dixon, and R. Carande. 2004. Space-based measurements of sheet-flow characteristics in the Everglades wetland, Florida. *Geophys. Res. Lett.* 31, doi:10.1029/2004GL020383.
- Yi, Y. 2000. OSU *stackfile*, Department of Civil and Environmental Engineering and Geodetic Science, Ohio State University, Columbus, Ohio.